

# Precursory seismicity pattern before strong earthquakes in Greece

Ioannis Baskoutas,<sup>1</sup>

George Anatoli Popandopoulos<sup>2</sup>

<sup>1</sup>Institute of Geodynamics, National Observatory of Athens; <sup>2</sup>Earthquake Planning and Protection Organization, Seismotectonic Division, Athens, Greece

## Abstract

The temporal variation of seismicity, based on the retrospective analyses of three seismic parameters *i.e.*, number of earthquakes, *b*-value and energy released, have shown significant changes. Their remarkable relation with strong earthquakes occurrence was formulated as a qualitative character precursory seismicity pattern, which were interpreted in terms of a strong earthquakes occurrence preparation phases. The main characteristic of this pattern is that permits the identification of two period of low and high probability for an earthquake occurrence, suggesting its utility in the current seismic hazard assessment, by the continuous monitoring of the temporal variation of the seismic parameters in a given area. This paper investigates the qualitative and quantitative characteristics of the proposed precursory seismicity pattern, before all strong earthquakes occurrence in Greece the time period 2000-2008.

## Introduction

Precursory seismicity changes have attracted the attention of researchers over the years and several types of patterns preceding large earthquakes have been reported in the literature. The majority of these precursory patterns were based on the analysis of the number of earthquakes and the quantitative and qualitative magnitude distribution in space and time worldwide.<sup>1-8</sup> In Greek territory Papadimitriou and Papazachos<sup>9</sup> have reported the evidence of precursory doughnut patterns in the Ionian Islands, while Papadopoulos<sup>10</sup> and collaborators propose a precursory seismicity pattern, in the north Aegean Sea, based on the spatial distribution clustering of strong earthquake.

Kanamori<sup>11</sup> has pointed out that although the nature of the precursory pattern varies from event to event, a common physical mechanism may be responsible which details are probably controlled by the tectonic environment and the heterogeneity of the medium.

Papadopoulos and Baskoutas<sup>12</sup> have introduced the new FastBEE algorithm for the seismic hazard assessment, based on the hypothesis that temporal changes of the seismicity reflects the influence of the previously mentioned factors on the strong earthquakes preparatory process, therefore the analysis of the temporal variation of the seismicity can reveal such influence. In this sense the respective FastBEE analysis tool was designed to obtain temporal variation curves of some basic seismicity parameters, which acts as seismic precursors, by the elaboration of common earthquake catalogue data.

The retrospective application of this algorithm<sup>13-15</sup> has shown that the obtained temporal variation series, over a long time interval, present significant changes temporal before strong earthquakes. These changes, because of their characteristic shapes and their relation to strong earthquake occurrence in the overwhelming majority of examined cases, can be considered as *prognostic anomalies* and because of their remarkable regularity can be considered as a qualitative precursory seismicity pattern. Distinct time intervals of these *prognostic anomalies* were interpreted by Popandopoulos and Baskoutas<sup>15</sup> in the term of the phases of the phenomenological *Consolidation Model* of the earthquake preparation process, proposed by Dobrovolsky.<sup>16</sup>

Given that the geodynamic regime in the Hellenic arc and trench system controls the physical process of strong earthquakes occurrence, this paper examine the qualitative and some quantitative characteristics of the above mentioned seismicity precursory pattern, before all the strong earthquakes, with magnitudes  $M > 6.0$  occurred in Greek territory in the time period 2000 to 2008.

## Brief description of the FastBEE algorithm

The seismicity parameters, calculated with the FastBEE algorithm are the number  $N$  of earthquakes per unit time, *b*-value and seismic energy released.

The number  $N$  of earthquakes in the Fast BEE algorithm is expressed as:

$$\log N(t) = \log \left( \sum_{i=t-w}^{n(t-w)} i \right) \quad (1)$$

where:

$i$  is the number of earthquakes, with magnitude  $M_s > M_{min}$ ;

$M_{min}$  is the minimum magnitude of the catalogue completeness;

$t$  is the time in months;

Correspondence: Ioannis Baskoutas, Institute of Geodynamics, National Observatory of Athens, P.O. Box 200 48, 118 10, Thessio, Athens, Greece. Tel. +30.210.3490174 - Fax: +30.210.3490180. E-mail: i.basko@noa.gr

Key words: seismic energy, *b*-value, temporal variation of seismicity, precursory seismicity pattern.

Received for publication: 31 May 2013.

Revision received: 11 September 2013.

Accepted for publication: 16 January 2014.

This work is licensed under a Creative Commons Attribution NonCommercial 3.0 License (CC BY-NC 3.0).

©Copyright I. Baskoutas and G.A. Popandopoulos, 2013

Licensee PAGEPress, Italy

Research in Geophysics 2014; 4:4899

doi:10.4081/rg.2014.4899

$w$  is the length of the smoothing window;  $n(t-w)$  is the number of earthquakes in the smoothing window time interval.

Given that the number of earthquakes in time is described by a Poisson distribution, the mean square error of the logarithm of the number  $N$  of earthquakes, is given by the relation:  $\sigma_{\lg N} = 0.4343/\sqrt{N}$ .

*b*-value of the frequency of the magnitude distribution relation, were calculated by means of the maximum likelihood<sup>17</sup> as:

$$b(t) = \lg \left[ 1 + \frac{N_{\Sigma}(t-w)}{\sum_{i=0}^n i \cdot N_{M_{min}+\Delta M}(t-w)} \right] / \Delta M \quad (2)$$

where:

$t$  is the time in months;

$N_{\Sigma}$  is the total number of earthquakes, with magnitude  $M_s > M_{min}$ ;

$M_{min}$  is the minimum magnitude of the catalogue completeness;

$N_{M_{min}+\Delta M}$  is the number of earthquakes in the  $i$ th magnitude;

$n = 1 + (M_{max} - M_{min}) / \Delta M$  is the number of the increment  $\Delta = 0.20$ .

The standard error of the *b*-value estimates is obtained by means of the relation:  $\sigma_b(t) = b(t) / \sqrt{N_{\Sigma}(t)}$

Finally, the seismic energy released, per unit of time, is expressed in the form  $\log E^{2/3}$  as:

$$\log E^{2/3}(t) = \log \left( \frac{1}{n(t-w)} \sum_{i=t-w}^{n(t-w)} E_i^{2/3} \right) \quad (3)$$

where:

$t$  is the time in months;

$n(t-w)$  is the number of earthquakes in the

smoothing window time interval;

$E_i^{2/3}$  is the seismic energy of the  $i^{\text{th}}$  earthquake in the time window  $w$ , which, for Greek territory, is equal to  $10^{1.5M_s+4.7, 18}$

Estimates of the temporal changes that exceed the confidence limits, in respect to the long-term observations, were taken as a measure of the statistical significance.

From the physical point of view, the quantity  $\log E_i^{2/3}$ , is proportional to the rate of accumulation of the dynamic ruptures in the strong earthquakes preparation process area,<sup>19,20</sup> and this may reflect the variations of the tectonic stress in the region of the observation.

The temporal variation series of all examined seismic parameters were obtained in two stages. In the first stage is created, a temporary seismic catalog data set, around the strong earthquake epicenter. Usually these areas dimensions, in the FastBEE algorithm is depending on the availability of the data and the purposes of the study, taking also into account the dimension of the examined seismogenic source. Based on the experience from previous retrospectively analyzed cases a rectangular area with size ranging from 80 to 120 km can fit adequately the purposes present study. Consequently the monthly arrays for all three examined parameters, using the following relations:

$$X_i = \sum_{i=1}^{n_i} x_i \quad X_i^2 = \sum_{i=1}^{n_i} x_i^2 \quad n_i = \sum_{i=1}^{n_i} i \quad (4)$$

where:

$x_i$  is the value of each parameter *i.e.*,  $\log N$ ,  $b$ -value and  $\log E_i^{2/3}$ ;

$n_i$  is the number of earthquakes in one month.

The creation of such monthly arrays allows obtaining the statistical estimates of the parameters by means of recursive formulas and according to the defined smoothing window. During the second stage, the monthly time series are smoothed, with a user defined smoothing window and with the resulting smoothed estimates assigned at the end of the smoothing window. As it is well known the use of a simple smoothing procedure is equivalent to the process of filtering with a rectangular shape filter.

In order to avoid the side lobes of the rectangular filter used, the smoothed time series were filtered again with another triangular-shape filter, of the same width. This new applied low-pass filter, allows the periods equal than the half of the smoothing window to pass without distortion. The new re-filtered estimates, this time are assigned at the center of the filtered window. The final output includes the temporal variation of all three examined seismic parameters, which each one appears as a complex of two superposed curves. The first thin violet curve represents the smoothed time series and the second bolder red line the filtered one. The standard errors for the  $b$ -value and the confidence limit  $1\sigma$  of the parameters  $\log N$  and  $\log E_i^{2/3}$  can be seen also, as lines parallel to their mean values in the examined time period.

## Qualitative temporal variation precursory seismicity pattern

The observed clear fluctuation of all parameters, over and above their relative mean values, forms consecutive relative minima and maxima. These changes are believed to reflect the changes in stress in the broader area and were interpreted in terms of qualitative character phenomenological cycle of earthquake preparation phases. Their remarkable and repeated relation with strong earthquakes occurrence, found in several retrospective analyses were considered as prognostic anomalies and the clear and repeated appearance as a qualitative character precursory seismicity pattern. The general trend of this pattern, in all three parameters, appears schematically in Figure 1 and its characteristics can be summarized as follow.

The temporal variation of the parameter  $\log N$ , shows, in the majority of the cases a clear decreasing phase toward to the relative mean value, in the examined time interval and below to the confidence level of 70%, reaching to a relative minimum. Usually the relative mean values, especially when the examined time interval is long enough, some how represent the background (*normal*) seismicity of a given region and the previously decreased behavior denote kind of *quiescence* period. This parameter usually reflects the fluctuation of the number of earthquakes despite the pres-

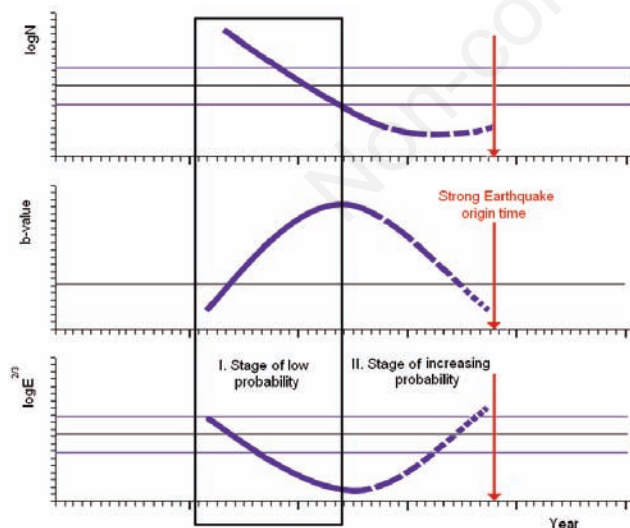


Figure 1. Characteristic FastBEE output schematic general trend of the temporal prognostic anomaly (solid blue lines) before a strong earthquake occurrence. The open rectangular parallelogram denotes the first, low probability stage, since the prognostic anomaly beginning, followed by a second higher probability stage, which conclude with the strong earthquake occurrence. Vertical red arrow shows the earthquake origin time.

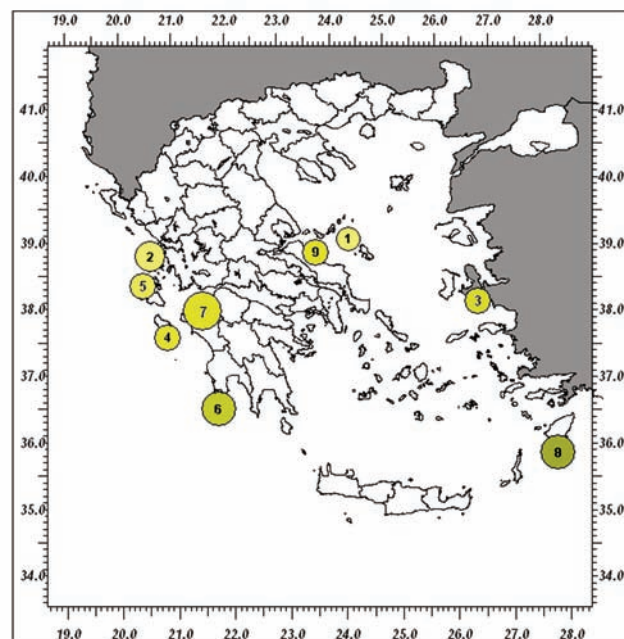


Figure 2. Map of seismic epicenters of the shallow strong earthquakes with magnitude  $M_S \geq 6.0$ , in the time period 2000-2008.

ent or the absence of a strong earthquake. In case of strong earthquake occurrence the influence of its aftershock activity can add information of the evaluation of the two other considered seismic parameters. In all examined cases, the preceded smaller magnitude events have not aftershock activity, in order to attribute the observed prognostic anomalies, in such kind of activity. Moreover it was found that the use of a declustered, for aftershocks, earthquake catalogue doesn't change the qualitative character of the observed precursory seismicity pattern. Parameter b-value instead shows at the beginning an increasing trend until it reaches a relative maximum. After that this parameter starts to decrease constantly toward to the relative mean value and even lower. Usually the strong earthquake occurrence coincides within this time interval and mostly at its later stage. Finally the fluctuation of the parameters  $\log E^{2/3}$ , in similarity with parameter  $\log N$  and contrary to the b-value behavior, is characterized by a gradual decrease toward to the relative mean value and even lower to the confidence limit. The inversion of this trend toward to the mean value, signalize the impending strong earthquake occurrence.

It was observed that the temporal evolution of the foresaid prognostic anomaly could be divided in two distinct temporal stages. During the

time evolution of the first stage the probability for a strong earthquake occurrence is very low, contrary with the beginning of the second stage the probability increases signaling thus an alarm period. As the temporal anomaly is approaching to its end the probability of occurrence became higher (dashed line in Figure 1). Among the three examined seismic parameters it was also found that b-value and the seismic energy releases in the form  $\log E^{2/3}$  are more informative in respect to the parameter  $\log N$ , although this last can add information when anomalous temporal variation appears in the seismicity of the region. Nonetheless parameter  $\log E^{2/3}$  seems to describe much better the observed temporal variation of the seismicity due to the temporal changes of the stress field influence, since this situation can be expressed better in the ambit of relatively greater size earthquake magnitudes *i.e.* greater than 3.5-3.8 those of smaller size.

## Data

In this analysis were investigated all shallow strong earthquakes, with magnitude  $M_s \geq 6.0$ , that occurred in Greek territory in the time period 2000-2008. The choice of this magni-

tude threshold, although arbitrary, represents according to Papazachos and Papazachou,<sup>18</sup> the lower magnitude of a destructive earthquake with a return period of about one year. The seismic data set used for each case, was taken from the Earthquake Catalogue of the Geodynamic Institute of the National Observatory of Athens (GINOA), Greece and they are homogeneous and complete for events with  $M \geq 3.5$  after 2000.<sup>3</sup> Table 1 reports the list of the examined strong earthquakes and their respective catalogue parameter. In the same table, the magnitudes taken for the U.S. Geological Survey/National Earthquake Information Center (USGS/NEIC) Global Hypocenters' Data Base System have been also reported, for a comparison. Figure 2 shows the epicenters of these strong earthquakes as numbered circles according to the serial numbers of Table 1 and with sizes proportional to their magnitude. The Skyros 2001, July 26,  $M_s=5.8$  earthquake, although its smaller size was also included in this study because it belongs to a cluster of eight (8) strong events, having epicenters very close to Greek capital Athens (Table 2), which have been occurred within 14 h, denoting thus a remarkable strong earthquakes activity. Moreover its main shock magnitude is reported as 6.5 according to NEIC Data Base.

**Table 1. Earthquakes catalogue parameters with magnitude  $M_S \geq 6.0$ , in the time period 2000-2008.**

s/n	Date	Origin time (UTC)	Latitude (degree)	Longitude (degree)	Depth (km)	Magnitude GINOA	Magnitude NEIC
1	2001 Jul 26	00:21	39.06	24.24	10	5.8	6.5 MwGS
2	2003 Aug 14	05:14	38.79	20.56	12	6.4	6.3 MwHRV
3	2005 Oct 17	05:45	38.13	26.59	29	6.0	5.5 MwHRV
4	2005 Oct 18	15:25	37.58	20.86	22	6.1	5.7 MwHRV
5	2007 Mar 25	13:57	38.34	20.42	15	6.0	5.7 MwGS
6	2008 Feb 14	10:09	36.50	21.78	41	6.7	6.9 MwGCMT
7	2008 Jun 8	12:25	37.98	21.51	25	7.0	6.4 MwGCMT
8	2008 Jul 15	03:26	35.85	27.92	56	6.7	6.4 MwGCMT
9	2008 Oct 14	02:06	38.85	23.62	24	6.1	5.2 MwGCMT

GINOA, Geodynamic Institute of the National Observatory of Athens; NEIC, National Earthquake Information Center.

**Table 2. List of the Skyros, July 26, 2001 earthquake aftershocks, with magnitude  $M_S \geq 5.0$ .**

s/n	Date	Origin time (UTC)	Latitude (degree)	Longitude (degree)	Depth (km)	Magnitude*
1	2001 Jul 26	00:21	39.06	24.24	10	5.8
2	2001 Jul 26	00:34	39.04	24.35	18	5.3
3	2001 Jul 26	02:01	39.10	24.31	21	5.0
4	2001 Jul 26	02:06	38.96	24.45	23	5.2
5	2001 Jul 26	02:09	38.92	24.52	24	5.3
6	2001 Jul 26	02:40	38.97	24.57	5	5.1
7	2001 Jul 26	04:53	39.06	24.38	22	5.1
8	2001 Jul 26	14:24	39.11	24.27	5	5.1

\*Parameters were taken from the catalog of Geodynamic Institute of National Observatory of Athens.

## Results

Each strong earthquake was examined for the presence of the foresaid temporal variation anomaly, before its occurrence and according to the characteristics of the previously outlined qualitative precursory seismicity pattern. Figure 3 shows the characteristic FastBEE output of the seismic parameters temporal variation and the origin time of the Skyros, Jul 26, 2001 Ms=5.8 strong earthquake as an example.

The visual inspection of this figure shows clearly the presence of the prognostic anomaly described previously preceding the strong earthquake. Precisely the parameter  $\log N$  start to decrease continuously after the middle of the year 1998, when it crosses the relative mean value equal to 1.32 denoting somehow a clear *quiescence period*, which lasts till the occurrence of the main shock. Simultaneously the parameters  $b$ -value and  $\log E^{2/3}$ , starts to increase and decreases respectively going through the first stage, of the low probability for an earthquake occurrence.

After one year (middle of the year 1999)

both reach the respective relative maximum and minimum, which denote the beginning of the second stage. This stage becomes critical in the middle of 2000 and especially when the  $\log E^{2/3}$  parameter crosses the lower confidence limit (70%) line, signaling the high probability of a strong earthquake, which occurred one year later *i.e.* July 26, 2000.

Application of this algorithm in different areas of Greece<sup>13,15</sup> and in India<sup>14</sup> has shown that parameters  $\log E^{2/3}$  is more informative in respect to the two others and more constant in respect to the  $b$ -value. For this reason we will consider this parameter in order to quantify the prognostic anomaly characteristics to compare with the rest of the examined cases and for further statistic analysis.

Figure 4 shows the polynomial regression estimates of the parameter  $\log E^{2/3}$  for the prognostic anomaly of the Skyros 2001 July 26, Ms=5.8 earthquake, with the respective equation and R-squared value. The regression equation and the respective R-squared value follow as:

$$y = 1^{-06}x^2 - 0.089x + 16 \quad (5)$$

and

$$R^2 = 0.67 \quad (6)$$

In the same way, were obtained the polynomial fittings for the rest of the examined cases, based on their shapes and their total durations on  $\log E^{2/3}$  seismic parameter prognostic anomalies, Figure 5. The mean value of statistical treatment of these anomalies can be expressed in terms of a mean polynomial equation of the form:

$$\log E = 2.01^{-01}x^2 - 8.13^{-02}x \quad (7)$$

Table 3 reports the duration of the prognostic anomalies in months, the polynomial fitting equation and the respective error for each examined case. From this table results that the mean duration of the prognostic anomaly measured in the parameter  $\log E^{2/3}$  is equal as  $45 \pm 28$  and range between a minimum of 17 to a maximum 73 months. Figure 6 shows the correlation between them is expressed in terms of a linear equation of the form:

$$T_{Dur} = 22.96Ms - 109.7 \quad (8)$$

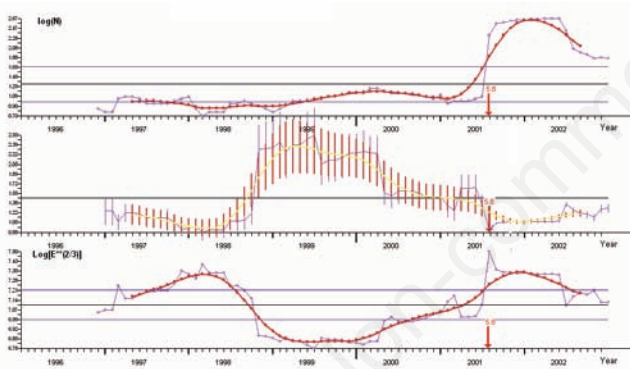


Figure 3. Temporal variation of the seismic parameters  $\log N[t]$ ,  $b$ -value and  $\log E^{2/3}$ , with their respective standard errors, for the Skyros 2001 July 26, Ms=5.8 strong earthquake. The numbered arrow perpendicular to the time axis denotes the earthquake origin time.

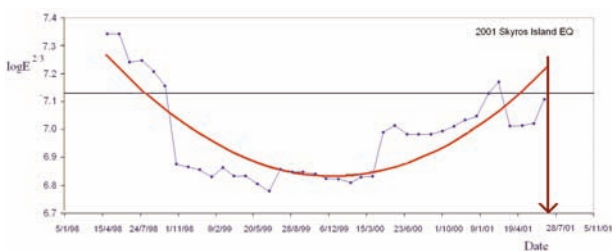


Figure 4. Smoothed temporal variation estimates of  $\log E^{2/3}$ , of the prognostic anomaly for the Skyros 2001 July 26, Ms=5.8 earthquake and the respective polynomial fitting line (red line).

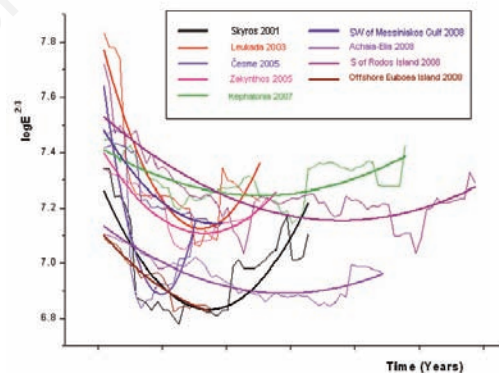


Figure 5. The shapes and the durations of the seismic parameter  $\log E^{2/3}$  prognostic anomalies for each examined strong earthquake and their respective polynomial fitting.

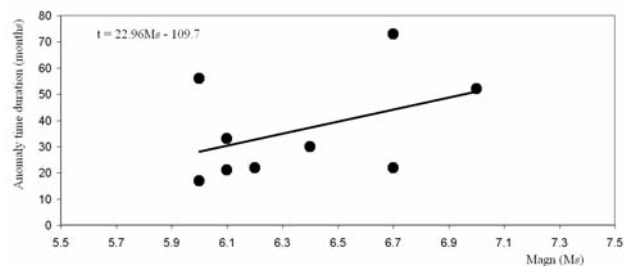


Figure 6. The dependence between magnitude of the examined strong earthquakes and total duration of the prognostic anomaly measured in the parameter  $\log E^{2/3}$ .

**Table 3. The duration of the prognostic anomalies, in the parameter  $\log E^{2/3}$  temporal variation and the magnitudes of the examined cases.**

s/n	Case of earthquake	Prognostic anomaly duration (months)	Equation	R <sup>2</sup>
1	Skyros 2001	38	$y = 1^{-06}x^2 - 0.09x + 16$	0.67
2	Leukada 2003	30	$y = 2^{-06}x^2 - 0.17x + 32$	0.78
3	Cesme 2005	17	$y = 9^{-07}x^2 - 0.069x + 13$	0.80
4	Zante 2005	33	$y = 2^{-07}x^2 - 0.016x + 32$	0.42
5	Kephalonia 2007	56	$y = 8^{-07}x^2 - 0.06x + 13$	0.89
6	S Messiniakos 2008	22	$y = 2^{-07}x^2 - 0.02x + 32$	0.70
7	Rodos 2008	73	$y = 2^{-07}x^2 - 0.02x + 32$	0.70
8	Achaia Elia 2008	52	$y = 2^{-06}x^2 - 0.16x + 31$	0.90
9	Evia 2008	21	$y = 4^{-07}x^2 - 0.03x + 68$	0.93

## Conclusions

The temporal variation analysis of a set of three seismicity parameters, using the FastBEE algorithm, was performed before all strong earthquakes in the time period 2000-2008. In all examined cases was found that their origin time falls within the time course of the second, high probability period, for a strong earthquake occurrence, and after the appearance of the preceding relative minimum of the temporal variation  $\log E^{2/3}$  curve, according to the proposed precursory seismicity pattern.

The prognostic anomalies observed in the parameter  $\log E^{2/3}$  curve, in all cases, were expressed in term of a polynomial fitting equation.

The duration of such precursory anomaly varies, from case to case, between 17 and 73 months and its dependence to the earthquake magnitude, although its small number of cases is rather low. This observation can be attributed to the influence of the geo-tectonic environment and the heterogeneity of the medium, factors that can accelerate or delay the earthquake occurrence.

The results suggest that the monitoring of the temporal variation of the seismicity in a given area, by the FastBEE algorithm, can contribute in the current seismic hazard assessment. The identification of the prognostic anomaly and its probability stages time evolution and especially the second high probability stage, can act as an alarm signal for an impending strong earthquake occurrence.

## References

- Mogi K. Earthquake prediction. New York, NY: Academic Press; 1985.
- Wyss M, Baer M. Seismic quiescence in the western Hellenic arc may foreshadow large earthquakes. *Nature* 1981;289:785-7.
- Smirnov VB, Baskoutas I, Zavyalov AD, et al. Space-time magnitude cut-off evolution of Greece Geodynamic Institute of National Observatory of Athens earthquake catalogue for 1964-2003. Proc. XXIX General Assembly of the ESC; Potzdam; 2004.
- Matthews MV, Reasenber PA. Statistical methods for investigating quiescence and other temporal seismicity patterns. *Pageoph* 1988;126:357-72.
- Keilis-Borok VI, Shebalin PN, Zaliapin IV. Premonitory patterns of seismicity months before a large earthquake: five case histories in Southern California. *Proc Natl Acad Sci U S A* 2002;99:16562-7.
- Tiampo KF, Rundle JB, McGinnis SA, Klein W. Pattern dynamics and forecast methods in seismically active regions. *Pageoph* 2002;159:2429-67.
- Matsumura S. Preparatory process reflected in seismicity-pattern change preceding the M=7 earthquakes off Miyagi prefecture. *Japan Earth Plan Space* 2006;58:1581-6.
- Sobiesiak M, Clark SA, Levander A, et al. Seismicity pattern and first b-value mapping of the Caribbean - South American plate boundary in North-eastern Venezuela. American Geophysical Union, Spring Meeting 2007, abstract #S33A-07. Available from: <http://adsabs.harvard.edu/abs/2007AGUSM.S33A.07S>
- Papadimitriou EE, Papazachos BC. Evidence for precursory seismicity patterns in the Ionian islands. *Earth Pred Res* 1985;3:95-3. [In Greece].
- Papadopoulos G, Ganas A, Plessa A. The Skyros earthquake [Mw 6.5] of 26 July 2001 and precursory seismicity pattern in the north Aegean Sea. *BSSA* 2002;92:1141-45.
- Kanamori H. The nature of seismicity patterns before large earthquakes. In: Simpson DW and Richards PG, eds. Earthquake prediction: an international review. Washington, DC: American Geophysical Union; 1981. pp 1-19.
- Papadopoulos G, Baskoutas I. New tool for the temporal variation analysis of seismic parameters. *Nat Hazards Earth Syst Sci* 2009;9:859-64.
- Baskoutas I, Papadopoulos G, Panopoulou G. Long temporal variation of seismic parameters for seismic patterns identification in Greece. *Bull Geol Soc Greece* 2004;XXXVI:1362-70.
- Baskoutas I, Popandopoulos AG, Prasanta C. Temporal variation of seismic parameters in the western part of the India-Eurasia plate collision zone. *Res Geophys* 2011;1:e3.
- Popandopoulos AG, Baskoutas I. Regularities in the time variations of seismic parameters and their implications for prediction of strong earthquakes in Greece. *Izvestiya Phys Solid Earth* 2011;47:974-94.
- Dobrovolsky IP. Teoriya podgotovki tektonicheskogo zemletryaseniya. [Theory of preparation of a tectonic earthquake]. Moscow: IFZ; 1991.
- Gusev AA. Earthquake prediction from statistical seismicity data. In: Fedotov SA, ed. Seismicity and seismic prediction, upper mantle properties and their relation to volcanism in Kamchatka. Novosibirsk: Nauka; 1974. pp 109-119.
- Papazachos B, Papazachou K. Earthquakes of Greece. Thessaloniki: Ziti Ed.; 2003.
- Keilis-Borok VI. On estimation of the displacement in an earthquake source and of source dimensions. *Ann Geofis* 1959;XII:205-14.
- Sadovskii MA, Pisarenko VF. On the dependence of the duration of earthquake preparation on its energy. *Dokl Akad Nauk SSSR* 1983;272:330-3.